

Boron Dipyrromethene Analogs with Phenyl, Styryl, and Ethynylphenyl Substituents: Synthesis, Photophysics, Electrochemistry, and Quantum-Chemical Calculations

Wenwu Qin,[†] Taoufik Rohand,[†] Wim Dehaen,[†] John N. Clifford,[†] Kris Driesen,[†] David Beljonne,[‡] Bernard Van Averbeke,[‡] Mark Van der Auweraer,[†] and Noël Boens^{*,†}

Department of Chemistry, Katholieke Universiteit Leuven, Celestijnenlaan 200f-bus 02404, 3001 Leuven, Belgium, and Laboratory for Chemistry of Novel Materials, University of Mons-Hainaut, Place du Parc 20, 7000 Mons, Belgium

Received: May 9, 2007; In Final Form: June 22, 2007

Seven fluorescent boradiazaindacene-based compounds with one or two phenyl, ethynylphenyl, and ethynylphenyl substituents at the 3- (or 3,5-) position(s) were synthesized via palladium-catalyzed coupling reactions with the appropriate 3,5-dichloroBODIPY derivative. The effect of the various substituents at the 3- (or 3,5-) position(s) on the spectroscopic and photophysical properties were studied as a function of solvent by means of UV/vis absorption, steady-state, and time-resolved fluorometry, and theoretical modeling. The emission maxima of the symmetrically 3,5-disubstituted dyes are shifted to longer wavelengths (by 30 to 60 nm) relative to the related asymmetrically 3,5-disubstituted ones. Introduction of styryl substituents causes the largest red shift in both the absorption and emission spectra. BODIPY derivatives with ethynylaryl groups also shift the spectral maxima to longer wavelengths compared to aryl-substituted ones but to a lesser degree than the styryl compounds. The quantum-chemical calculations confirm these trends and provide a rationale for the spectral shifts induced by substitution. The fluorescence quantum yields of the ethynylaryl and ethynylaryl analogs are significantly higher than those of the aryl-substituted dyes. The 3,5-diethynylaryl dye has the highest fluorescence quantum yield (~ 1.0) and longest lifetime (around 6.5 ns) among the BODIPY dyes studied. The differences in the photophysical properties of the dyes are also reflected in their electrochemical properties where the symmetrically 3,5-disubstituted dyes display much lower oxidation potentials when compared to their asymmetric counterparts.

1. Introduction

The study of the spectroscopic and photophysical properties of fluorescent dyes is of great scientific and technological importance because of the significant implications in photonics and in the development of new fluorescent chemosensors.¹ Because of their favorable properties, 4,4-difluoro-4-bora-3a,4a-diaza-*s*-indacene (BODIPY, difluoroborondipyrromethene)^{2,3} derivatives have become preferred fluorophores in new fluorescent probes that have found widespread applications in numerous fields of modern medicine and science.⁴ The excellent qualities of BODIPY comprise relatively high molar absorption coefficients ($\epsilon > 50\,000\text{ M}^{-1}\text{ cm}^{-1}$) and fluorescence quantum yields ϕ_f (often approaching 1.0), narrow emission bandwidths with high peak intensities, elevated stability toward light and chemicals, and the extra feature that they can be photoexcited with visible light (excitation/emission wavelengths above 500 nm). Moreover, they are open to structural modification so that their spectroscopic properties can be fine-tuned by introducing suitable substituents at the right positions.

While there are several potential sites on the BODIPY chromophore where functionalization can be done, appropriate substituents at the 3,5-positions can shift the excitation and emission bands as a function of solvent polarity/polarizability. Recently, we reported that the chlorine atoms of 3,5-dichloro-

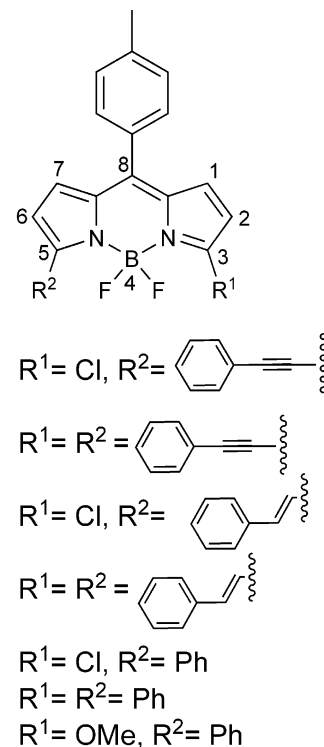


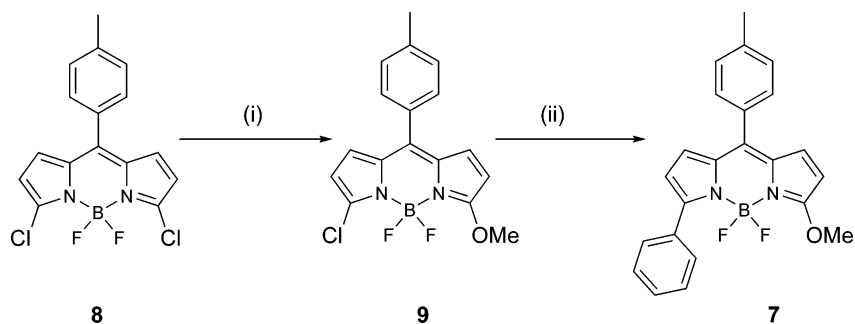
Figure 1. Chemical structures of the BODIPY dyes 1–7.

8-(4-tolyl)-4,4-difluoro-4-bora-3a,4a-diaza-*s*-indacene (**8**) can be substituted by oxygen, nitrogen, sulfur, and carbon nucleo-

* To whom correspondence should be addressed. E-mail: Noel.Boens@chem.kuleuven.be. Fax: +32-16-327 990.

[†] Katholieke Universiteit Leuven.

[‡] University of Mons-Hainaut.

SCHEME 1: Synthesis of the BODIPY Derivatives **7** and **9**^a

^a Reaction conditions: (i) NaOMe/methanol/rt/30 min; (ii) phenylboronic acid/Pd(PPh₃)₄/Na₂CO₃/DME/MW/150 °C/20 min.

philes.⁵ Furthermore, palladium-catalyzed coupling reactions (Stille, Suzuki, Heck, and Sonogashira) on 3,5-dichloroBODIPY analogs such as **8** are a practical way for preparing asymmetrically (**1**, **3**, **5**, **7**) and symmetrically (**2**, **4**, **6**) substituted, conjugated BODIPY derivatives (Figure 1).⁶

In this paper, we report the synthesis of a new asymmetrically 3,5-disubstituted boron dipyrromethene derivative (Scheme 1) and investigate the spectroscopic properties and the photophysical characteristics of seven boradiazaindacene-based compounds with one or two phenyl, styryl, and ethynylphenyl substituents at the 3- (and 5-) position(s). Using UV/vis absorption and steady-state and time-resolved fluorescence spectroscopy, the effect of the molecular structure on the solvent-dependent spectroscopic properties is studied. From these experiments, we were able to determine the wavelengths of the spectral maxima (λ_{abs} , λ_{ex} , λ_{em}), the full width at half-maximum of the absorption band (fwhm(abs)), the Stokes shifts ($\Delta\bar{\nu}$), the fluorescence quantum yields (ϕ_f) and lifetimes (τ), and the rate constants of fluorescence (k_f) and nonradiative (k_{nr}) deactivation. The photophysical characteristics of the studied BODIPY analogs strongly depend on the nature of the 3,5-substituents (phenyl, ethynylphenyl, and ethynylphenyl). Semiempirical quantum-chemical calculations performed for these derivatives are consistent with the experimental trends and provide useful insight into the relationship between the type of the substituents and the nature of the lowest optical electronic excitations.

2. Experimental Section and Theoretical Methods

2.1. Materials. All solvents for the spectroscopic measurements were of spectroscopic grade and were used without further purification. The chemicals used for the synthesis were used as received. Dichloromethane (pa), however, was dried over molecular sieves. Boron trifluoride etherate contained ca. 48% BF₃.

2.2. Syntheses. ¹H and ¹³C NMR spectra were recorded at room temperature on a Bruker Avance 300 instrument operating at a frequency of 300 MHz for ¹H and 75 MHz for ¹³C. ¹H NMR spectra were referenced to tetramethylsilane (0.00 ppm) as an internal standard. Chemical shift multiplicities are reported as s = singlet, d = doublet, q = quartet, and m = multiplet. ¹³C spectra were referenced to the CDCl₃ (77.67 ppm) signal. Mass spectra were recorded on a Hewlett-Packard 5989A mass spectrometer (EI mode and CI mode). High-resolution mass data were obtained with a Kratos MS50TC instrument. Melting points were taken on a Reichert Thermovar and are uncorrected.

3,5-Dichloro-8-(4-tolyl)-4,4-difluoro-4-bora-3a,4a-diaza-s-indacene (**8**) is the starting compound for the synthesis of BODIPY derivatives **7** and **9** (Scheme 1). The detailed synthetic

procedures for these compounds are described below. The syntheses of compounds **1–6** have been reported recently.⁶

3-Chloro-5-methoxy-8-(4-tolyl)-4,4-difluoro-4-bora-3a,4a-diaza-s-indacene (9). Under argon atmosphere, 200 mg (0.57 mmol) of 3,5-dichloro-8-(4-tolyl)-4,4-difluoro-4-bora-3a,4a-diaza-s-indacene **8** was dissolved in 50 mL of absolute methanol. Within 10 min, 2 equiv of freshly prepared sodium methoxide in methanol was added dropwise while the reaction mixture was stirred. Stirring was continued at room temperature for 30 min; the reaction was then quenched with 50 mL of water and extracted with dichloromethane (3 × 40 mL). The organic layer was dried (MgSO₄) and evaporated under reduced pressure, and the residue was purified by column chromatography over silica gel using ethyl acetate–petroleum ether (3:7, v/v) as eluent to afford 128.1 mg (65% yield) of **9** as red crystals. Mp: 219 °C. ¹H NMR (CDCl₃): δ 7.37 (d, 2H, J = 8.0 Hz), 7.29 (d, 2H, J = 8.0 Hz), 6.96 (d, 1H, J = 4.8 Hz), 6.61 (d, 1H, J = 4 Hz), 6.28 (d, 1H, J = 4 Hz), 6.14 (d, 1H, J = 4.8 Hz), 4.14 (s, 3H, OCH₃), 2.45 (s, CH₃). ¹³C NMR (CDCl₃, 75 MHz): δ 169.71 (s), 141.04 (d), 140.81 (s), 137.55 (s), 135.43 (s), 132.61 (s), 130.74 (d), 130.48 (d), 130.37 (s), 129.43 (s), 126.57 (d), 115.77 (d), 104.54 (d), 59.55 (q), 21.76 (q). LRMS (EI 70 eV) [m/z (%): 346 (M⁺, 100), 331 (90), 312 (41), 297 (52), 333 (35). HRMS: calcd for C₁₇H₁₄BClF₂N₂O, 346.085 5; found, 346.085 8.

3-Methoxy-5-phenyl-8-(4-tolyl)-4,4-difluoro-4-bora-3a,4a-diaza-s-indacene (7). To a solution of **9** (100 mg, 0.29 mmol) in 1,2-dimethoxyethane (DME, 3 mL) were added phenylboronic acid (71.7 mg, 0.58 mmol), Na₂CO₃ (92.2 mg, 0.87 mmol), and a catalytic amount of Pd(PPh₃)₄ (8.6 mg, 0.008 mmol). The reaction mixture was stirred under microwave (MW) irradiation for 20 min at 150 °C and 200 W. The reaction was then quenched by addition of H₂O (30 mL), and the aqueous layer was extracted with CH₂Cl₂ (3 × 40 mL). The organic layer was dried (MgSO₄) and the solvent evaporated under reduced pressure. The crude product was purified by chromatography on silica gel, eluting with dichloromethane to give 76.6 mg (68% yield) of **7** as a reddish crystals. Mp: 258–259 °C. ¹H NMR (CDCl₃): δ 7.9 (d, 2H, J = 8.2 Hz), 7.46–7.34 (m, 5H, aromatic), 7.31 (d, 2H, J = 8.2 Hz), 6.93 (d, 1H, J = 4.6 Hz), 6.74 (d, 1H, J = 3.6 Hz), 6.53 (d, 1H, J = 3.6 Hz), 6.08 (d, 1H, J = 4.6 Hz), 4.08 (s, 3H, OCH₃), 2.46 (s, 3H, CH₃). ¹³C NMR (CDCl₃, 75 MHz): δ 168.3 (s), 141.4 (s), 140.0 (s), 135.2 (s), 133.5 (d), 133.3 (s), 131.1 (s), 130.8 (d), 130.4 (d), 129.5 (d), 129.2 (d), 128.9 (d), 128.5 (s), 128.0 (s), 127.5 (d), 118.2 (d), 102.9 (d), 58.8 (q), 21.7 (q). LRMS (EI 70 eV) [m/z (%): 388 (M⁺, 100), 373 (44), 333 (29), 254 (11), 200 (14), 181 (12), 167 (11), 149 (34). HRMS: calcd for C₂₃H₁₉BF₂N₂O, 388.155 8; found, 388.155 6.

TABLE 1: Photophysical Properties of 1 and 2 in Several Solvents

BODIPY	solvent ^a	λ_{abs} (max/nm)	λ_{em} (max/nm)	λ_{ex} (max/nm)	fwhm(abs) (cm ⁻¹)	$\Delta\bar{\nu}$ (cm ⁻¹)	ϕ_f	τ^b (ns)	k_f (10 ⁸ s ⁻¹)	k_{nr} (10 ⁸ s ⁻¹)
1	toluene	566	577	566	851	337	0.91	4.45	2.0	0.2
	CHCl ₃	564	577	564	924	399	0.95	4.73	2.0	0.1
	cyclohexane	564	575	564	697	339	1.00	4.31	2.3	0
	1,4-dioxane	562	575	562	897	402	0.97	4.43	2.2	0.1
	THF	560	573	559	869	405	0.84	4.24	2.0	0.4
	EtOAc	558	571	558	879	408	0.83	4.34	1.9	0.4
	MeOH	556	569	556	882	411	0.98	4.25	2.3	0.
2	toluene	614	629	614	1112	388	1.00	6.18	1.6	0
	CHCl ₃	614	628	614	972	363	1.00	6.66	1.5	0
	cyclohexane	615	626	615	861	286	1.00	6.58	1.5	0
	1,4-dioxane	612	626	612	1036	365	1.00	6.44	1.6	0
	THF	610	625	610	955	393	0.99	6.62	1.5	0
	EtOAc	607	621	607	1024	371	1.00	6.74	1.5	0
	MeOH	605	622	605	1030	452	1.00	6.51	1.5	0

^a The solvents are ordered (from top to bottom) according to decreasing polarizability (as measured by the refractive index n). ^b The standard errors on all lifetimes τ are ≤ 10 ps.

2.3. Steady-State Spectroscopy. UV/vis absorption spectra were recorded on a Perkin-Elmer Lambda 40 UV/vis spectrophotometer, while, for the fully corrected steady-state excitation and emission spectra, a SPEX Fluorolog was employed. All absorption and excitation/emission spectra were recorded at 20 °C using non-degassed samples. For each dye in a specific solvent, three or four absorption, excitation, and emission spectra were measured as a function of dye concentration. Since the spectra are recorded digitally and the peaks are relatively narrow, the maxima can be determined not only from visual inspection but also via the analysis–calculus–integrate menu of the Origin software. The error on the wavelength of the maximum is usually 1–2 nm. For the determination of the fluorescence quantum yields (ϕ_f), only dilute solutions with an absorbance below 0.1 at the excitation wavelength λ_{ex} were used. Rhodamine 6G in H₂O ($\lambda_{\text{ex}} = 488$ nm, $\phi_f = 0.76$) for **5** and **7** and Cresyl violet in methanol ($\lambda_{\text{ex}} = 546$ nm, $\phi_f = 0.55$) for **1–4** and **6** were used as fluorescence standards.⁷ The ϕ_f values reported in this work are the averages of multiple (generally 3), fully independent measurements. The majority of the ϕ_f determinations was done using non-degassed samples. To check the influence of dissolved oxygen on ϕ_f , several samples, degassed via successive freeze–pump–thaw cycles, were measured. The obtained ϕ_f values were within experimental error equal for aerated and degassed samples, in agreement with results for other BODIPY derivatives.⁸ That O₂ did not influence the measured fluorescence quantum yields is further evidenced by the unit ϕ_f values for compound **2**, which also has the highest fluorescence lifetime τ (Table 1). Indeed, if dissolved oxygen would quench the fluorescence, it would be impossible to have quantum yields of 1.0. In all ϕ_f determinations, correction for the refractive index was applied.

2.4. Time-Resolved Spectroscopy. Fluorescence decay traces of the fluorescent dyes **1–7** were recorded at several emission wavelengths by the single-photon timing method.⁹ Details of the instrumentation used and experimental procedures have been described elsewhere.¹⁰ The samples were excited at 488 nm for **7**, at 543 nm for **1**, **3**, and **6**, and at 580 nm for **2** and **4** with a repetition rate of 4.09 MHz for 488 nm and 8.18 MHz for 543 and 580 nm. Fluorescence decay histograms were collected in 4096 channels with a time increment/channel of 5 ps using 10 × 10 mm optical path length cuvettes. The absorbance at the excitation wavelength was always below 0.1. All lifetime measurements were performed on samples that were degassed by consecutive freeze–pump–thaw cycles. Histograms of the instrument response function were recorded using a LUDOX

scatterer. The full width at half-maximum of the instrument response function was ~ 60 ps. All measurements were done at 20 °C.

The fitting parameters were determined by minimizing the global, reduced χ -square χ_g^2 :

$$\chi_g^2 = \sum_l^q \sum_i w_{li} (y_{li}^o - y_{li}^c)^2 / \nu \quad (1)$$

Here the index l sums over q experiments and the index i sums over the appropriate channel limits for each individual experiment. y_{li}^o and y_{li}^c denote respectively the observed and calculated (fitted) values corresponding to the i th channel of the l th experiment, and w_{li} is the corresponding statistical weight. ν represents the number of degrees of freedom for the entire multidimensional fluorescence decay surface.

The statistical criteria to assess the quality of the fit included both graphical and numerical tests and have been described elsewhere.^{9c,11} The decays were analyzed first individually by a (multi)exponential decay law in terms of decay times τ_i and their associated preexponential factors α_i . The final curve-fitting was done by global analysis in which decays recorded at four different observation wavelengths (570, 580, 590, and 600 nm for **1**; 620, 630, 640, and 650 nm for **2**; 580, 590, 600, and 610 nm for **3** and **6**; 630, 640, 650, and 660 nm for **4**; 550, 560, 570, and 580 nm for **7**) were described by a single-exponential decay function with a linked lifetime τ and local (nonlinked) preexponentials α . The quality of the fit was judged for each fluorescence decay trace separately as well as for the global fluorescence decay surface. All curve fittings presented here had χ^2 values below 1.1.

For the single-exponential fluorescence decays, the rate constants of fluorescence (k_f) and nonradiative (k_{nr}) deactivation were calculated from the measured fluorescence quantum yield ϕ_f and lifetime τ according to eqs 2 and 3:

$$k_f = \phi_f / \tau \quad (2)$$

$$k_{\text{nr}} = (1 - \phi_f) / \tau \quad (3)$$

2.5. Electrochemistry. Electrochemical data were obtained using an Autolab PGSTAT12 potentiostat and a standard three-electrode cell (platinum working and counter electrodes and an Ag/AgCl reference) at scan rates of 200 mV s⁻¹. Voltammograms were recorded at room temperature in a solution of 0.1 M tetrabutylammonium hexafluorophosphate ((TBA)PF₆) as the

supporting electrolyte in dichloromethane. All solutions were purged with argon prior to measurement.

2.6. Computational Details. Molecular properties in the gas phase were obtained using semiempirical quantum-chemical methods. The ground-state/excited-state geometries of the BODIPY derivatives were first computed at the AM1//AM1/CI level.¹² These structures were subsequently used as input for electronic excited-state calculations performed at the INDO/SCI level.¹³ The highest 40 occupied and lowest 40 unoccupied molecular orbitals were included in the SCI active space.

On the basis of the optimized excited-state geometries, the (gas-phase) radiative lifetimes of the different derivatives were computed with the Einstein coefficient for spontaneous emission:

$$\tau^{-1} = \frac{8\pi^2\nu^3}{3\epsilon_0c^3\hbar} |\mu|^2 \quad (4)$$

Here μ is the transition dipole moment from the lowest excited-state to the ground state (in Debye) and ν denotes the corresponding excitation frequency (in Hz).

3. Results and Discussion

Compounds **1–7** were synthesized by palladium-catalyzed C–C coupling reactions with compound **8** as starting compound. This synthetic methodology is extremely useful for the formation of asymmetric (**1**, **3**, **5**, and **7**) and symmetric (**2**, **4**, and **6**) BODIPY analogs (Figure 1) with different substituents at the 3,5-positions. Because dyes **1** and **2**, synthesized via Sonogashira coupling of phenylacetylene with **8**,⁶ are the first reported 3-ethynylphenyl- and 3,5-diethynylphenyl-substituted boradiazaindacene derivatives, we report their photophysical properties first.

3.1. Spectroscopic Properties of the Ethynylphenyl-Substituted Derivatives **1 and **2**.** Figure 2 shows the UV/vis absorption and fluorescence emission spectra of **1** dissolved in several solvents. The absorption spectra are of shape similar to those described of the BODIPY dyes,^{8,14–18} with an intense absorption band at ~ 560 nm and a shoulder at the short wavelength side. The absorption spectra are hardly affected by solvent polarity, the maximum being blue-shifted (by 10 nm) when the solvent is changed from toluene (566 nm) to methanol (556 nm), consistent with the absorption spectroscopic behavior of BODIPY chromophores. This small shift reflects the polarizability of the solvent. The absorption spectra of **1** all show narrow spectral bandwidths with two absorption maxima: (1) the 0–0 band of a strong S_0 – S_1 transition with a maximum ranging from 556 to 566 nm; (2) the (more or less pronounced) shoulder on the high-energy side, which is attributed to the 0–1 vibrational band of the same transition. Additionally, a weaker, broad absorption band—attributed to the S_0 – S_2 transition—is found between 380 and 410 nm, the position of which is not appreciably affected by solvent polarity. The full width at half-maximum (fwhm(abs)) of the main S_0 – S_1 band varies slightly with the solvent (from 697 cm^{-1} in cyclohexane to 924 cm^{-1} in chloroform). However, there is no systematic trend observable for fwhm(abs) as a function of solvent. Table 1 summarizes the photophysical data of **1** in several solvents. The wavelengths of the absorption maxima of **1** are approximately 50–60 nm red-shifted compared to conventional BODIPY derivatives.^{8,14–18}

Compound **1** also shows the typical emission features of boradipyrromethene^{8,14–18} (Figure 2), that is, a narrow, slightly Stokes-shifted band of mirror image shape. The fluorescence maxima are blue-shifted with decreasing solvent polarizability (from 577 nm in toluene to 569 nm in methanol, Table 1). The

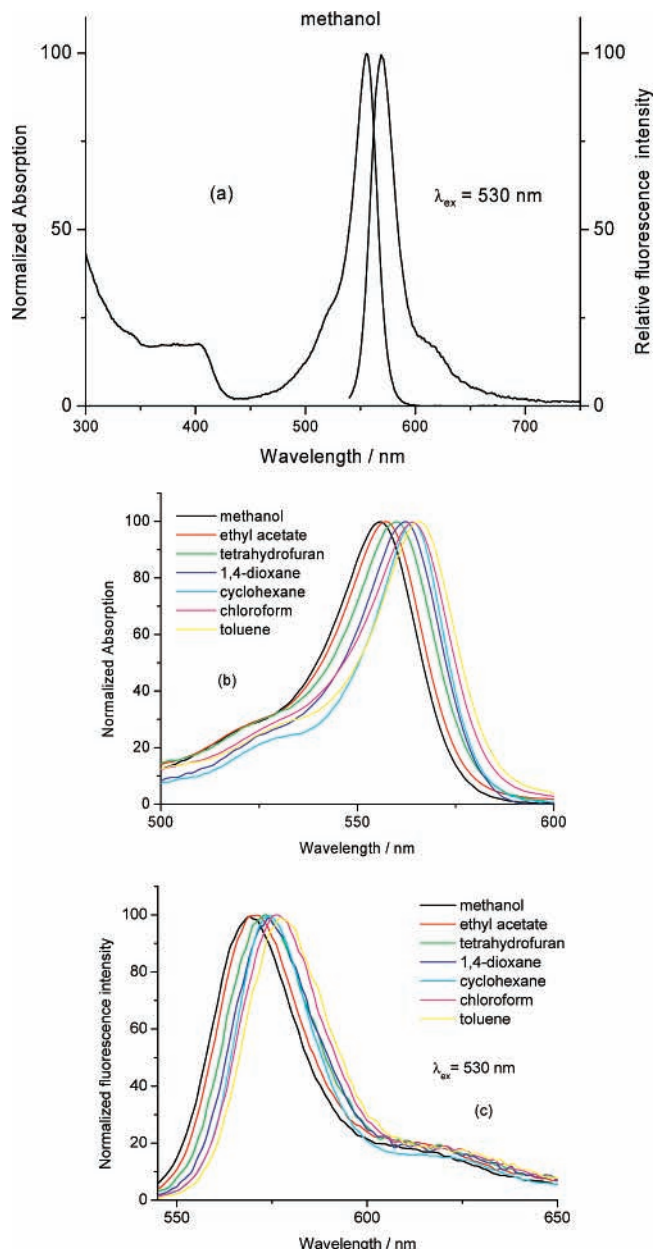


Figure 2. (a) Normalized absorption and fluorescence emission ($\lambda_{\text{ex}} = 530$ nm) spectra of **1** in methanol. (b) Enlargement of the main absorption peak of **1** in several solvents to emphasize the solvatochromic shifts. (c) Enlargement of the main fluorescence emission peak of **1** in several solvents to emphasize the solvatochromic shifts. The excitation wavelength is 530 nm. The intensities in this figure are normalized to the same value at the wavelength of maximum intensity.

fluorescence quantum yields ϕ_f of **1** are very high in all solvents used ($0.83 \leq \phi_f \leq 1.00$), with the lower values found for the more polar, aprotic solvents EtOAc and THF.

The steady-state absorption and fluorescence emission spectra of **2** are displayed in Figure 3. The absorption and emission spectra of **2** are of shape similar to those of previously described borodipyrromethene dyes.^{8,14–18} Compared to the 3-ethynylphenyl-substituted compound **1**, the absorption and emission wavelength maxima of the 3,5-diethynylphenyl-substituted dye **2** are red-shifted by ~ 50 nm to around 610 and 625 nm, respectively. These shifts reflect the fact that the extra ethynyl substituent at the 5-position increases the conjugation to the boradiazaindacene core (see modeling section). The ϕ_f values of **2** are extremely high (1.0) and independent of the solvent. The absorption spectral bandwidths of **1** and **2** are similar [the

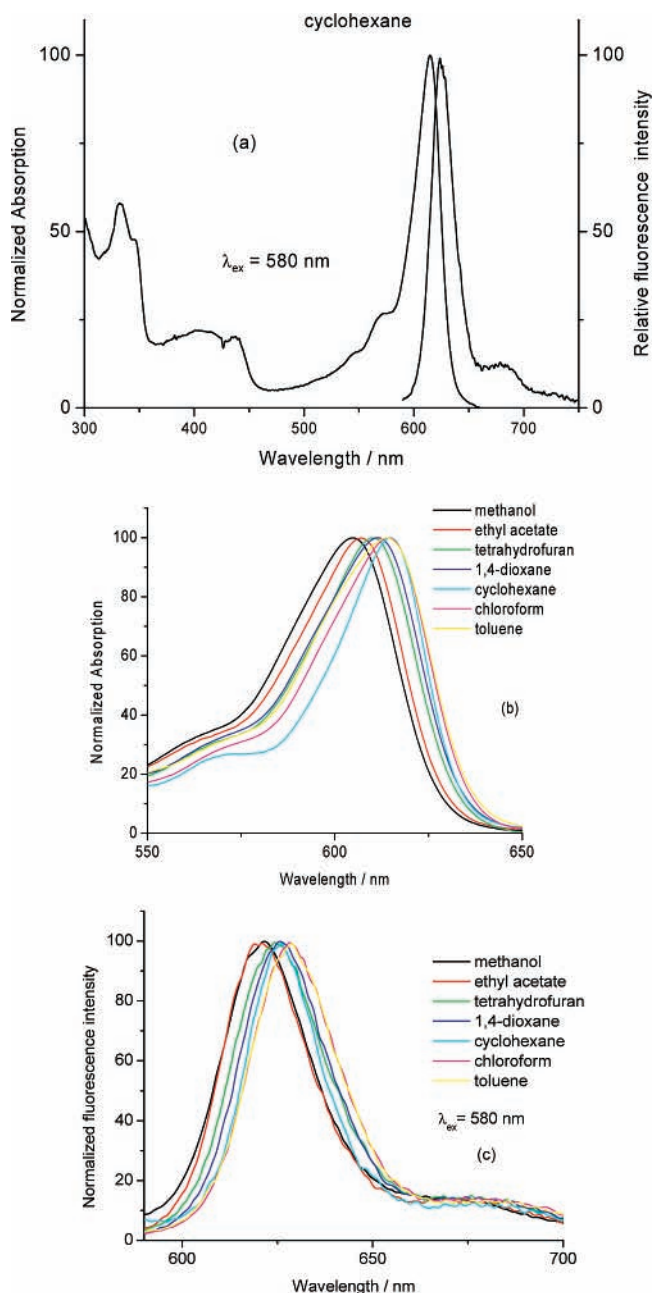


Figure 3. (a) Normalized absorption and fluorescence emission ($\lambda_{\text{ex}} = 580$ nm) spectra of **2** in cyclohexane. (b) Enlargement of the main absorption peak of **2** in several solvents to accentuate the solvatochromic shifts. (c) Enlargement of the main fluorescence emission peak of **2** in several solvents to accentuate the solvatochromic shifts. The excitation wavelength is 580 nm. The intensities in this figure are normalized to the same value at the wavelength of maximum intensity.

average fwhm(abs) obtained in the various solvents equals $(8.6 \pm 0.7) \times 10^2 \text{ cm}^{-1}$ for **1** and $(10.0 \pm 0.8) \times 10^2 \text{ cm}^{-1}$ for **2**. As for **2**, no systematic trend is observable for fwhm(abs) as a function of solvent.

To study the time-resolved fluorescence of **1** and **2**, fluorescence decay histograms in different solvents were collected as a function of emission wavelength. All fluorescence decay profiles of **1** and **2** could be described by a single-exponential fit in all the solvents used. The lifetimes τ estimated via single-curve analysis were independent of the observation wavelength. Simultaneous (or global) curve-fitting of the fluorescence decay surface with τ linked as a function of the observation wavelength confirmed that the decays are indeed single-exponential and do not depend on the emission wavelength. The estimated fluo-

rescence lifetimes τ are compiled in Table 1. The lifetime values of **1** are nearly solvent independent with a mean value for $\tau = 4.4 \pm 0.2$ ns. For **1**, the k_f values calculated according to eq 2 yield an average value for $k_f = (2.1 \pm 0.2) \times 10^8 \text{ s}^{-1}$. The τ values obtained for **2** ($\tau = 6.5 \pm 0.2$ ns) are among the highest ever measured for “classical” difluoroboradipyrromethene derivatives.^{3,19} Replacement of the F atoms in difluoroboradipyrromethene with ethynylaryl subunits (aryl = tolyl, anthryl, pyrenyl, or perylenyl) results in B-substituted dyes with even higher lifetimes.^{3,20} Substitution of the fluorines of the boron atom in the BODIPY unit by 4-(1-pyrenyl)-butan-1-ol yields a dye with a 14.6 ns fluorescence lifetime in dichloromethane.³ The lifetime values of **2** also are independent of the solvent. For **2**, the average k_f value is found to be $(1.53 \pm 0.05) \times 10^8 \text{ s}^{-1}$.

3.2. Spectroscopic Properties of the Styryl-Substituted Analogs 3 and 4. BODIPY analogs **3** and **4** were synthesized via the Heck reaction between styrene and **8**.⁶ 3-Ethenylaryl-substituted boron dipyrromethene derivatives have been synthesized before via an alternative synthesis path by a condensation reaction between an appropriately substituted benzaldehyde and suitable 3,5-dimethyldifluorodiazaindacene derivatives.²¹ Two 3,5-distyrylBODIPY dyes have been prepared by a condensation reaction of 2-styrylpyrrole with an aromatic aldehyde.²²

The absorption and emission spectra of **3** and **4** are of shape similar to those of similar, previously described boron dipyrromethene dyes.^{21,22} Introduction of styryl groups (at the 3-position in **3** and at the 3,5-positions in **4**) causes the largest bathochromic shift in both the absorption and emission spectra of the investigated BODIPY compounds **1–7**. For example, the absorption and emission maxima [$\lambda_{\text{abs}}(\text{max})$ and $\lambda_{\text{em}}(\text{max})$, respectively] of asymmetric **3** are red-shifted by ~ 10 nm compared to **1**, whereas $\lambda_{\text{abs}}(\text{max})$ and $\lambda_{\text{em}}(\text{max})$ of **4** are red-shifted by ~ 20 nm compared to the corresponding symmetrically 3,5-disubstituted dye **2** (Table 2). The absorption spectral bandwidths fwhm(abs) of **3** and **4** are quite narrow [the mean fwhm(abs) value in the various solvents equals $(8.8 \pm 0.4) \times 10^2 \text{ cm}^{-1}$ for **3** and $(6.8 \pm 0.2) \times 10^2 \text{ cm}^{-1}$ for **4**]. It should be noted that the smaller fwhm(abs) of **4** compared to **3** corresponds to a smaller Stokes shift $\Delta\bar{\nu}$, suggesting a smaller difference in equilibrium coordinates in S_0 and S_1 . This is also in agreement with the smaller values of k_{nr} observed for **4** compared to **3** (see below). The emission spectra of **4** extend into the near-infrared spectral region [$\lambda_{\text{em}}(\text{max}) = \sim 640\text{--}650$ nm]. The quantum yield ϕ_f and lifetime τ for asymmetric **3** decrease with increasing solvent polarity when the solvent is changed from cyclohexane ($\epsilon = 2.0$, $\phi_f = 0.72$, and $\tau = 3.64$ ns) to methanol ($\epsilon = 32.6$, $\phi_f = 0.55$, and $\tau = 3.16$ ns). Conversely, the ϕ_f (0.90 ± 0.05) and τ (4.5 ± 0.2 ns) values of the symmetric dye **4** are nearly independent of the solvent. The photophysical characteristics [$\lambda_{\text{abs}}(\text{max})$, $\lambda_{\text{em}}(\text{max})$, ϕ_f , and τ] of **3** and **4** are very close to similar, previously reported compounds.^{21,22} For **3**, the k_f values in the various solvents calculated according to eq 2 yield an average value of $(1.7 \pm 0.1) \times 10^8 \text{ s}^{-1}$, while for **4** the corresponding k_f value is found to be $(2.0 \pm 0.1) \times 10^8 \text{ s}^{-1}$. For **3**, the k_{nr} values are systematically larger in the more polar solvents. For **4**, the k_{nr} values are much smaller those of **3** and, furthermore, it is impossible to perceive a trend.

3.3. Spectroscopic Properties of the Phenyl-Substituted Dyes 5–7. Dyes **5** and **6** were synthesized via Stille coupling between tetraphenyltin and **8**.⁶ The synthesis of **7** (Scheme 1) involves a conventional substitution with methoxide followed by a palladium-catalyzed Suzuki coupling with phenylboronic

TABLE 2: Photophysical Properties of 3 and 4 in Several Solvents

BODIPY	solvent ^a	λ_{abs} (max/nm)	λ_{em} (max/nm)	λ_{ex} (max/nm)	fwhm(abs) (cm ⁻¹)	$\Delta\bar{\nu}$ (cm ⁻¹)	ϕ_{f}	τ^b (ns)	k_{f} (10 ⁸ s ⁻¹)	k_{nr} (10 ⁸ s ⁻¹)
3	toluene	572	588	572	830	476	0.69	3.68	1.9	0.8
	CHCl ₃	571	585	571	898	419	0.68	3.98	1.7	0.8
	cyclohexane	569	581	569	875	363	0.72	3.64	2.0	0.8
	1,4-dioxane	569	582	569	904	393	0.60	3.68	1.6	1.1
	THF	568	581	568	940	394	0.56	3.45	1.6	1.3
	EtOAc	565	580	565	854	458	0.57	3.43	1.7	1.3
	MeOH	564	579	564	824	459	0.55	3.16	1.7	1.4
4	toluene	637	649	637	695	290	0.93	4.48	2.1	0.2
	CHCl ₃	635	647	635	699	292	0.93	4.63	2.0	0.2
	cyclohexane	630	642	630	660	297	0.96	4.37	2.2	0.1
	1,4-dioxane	633	646	633	677	318	0.86	4.31	2.0	0.3
	THF	632	645	632	682	319	0.82	4.09	2.0	0.4
	EtOAc	628	641	628	664	323	0.89	4.77	1.9	0.2
	MeOH	626	639	626	693	325	0.92	4.54	2.0	0.2

^a The solvents are ordered according to decreasing polarizability (with the refractive index n as criterion). ^b The standard errors on all lifetimes τ are ≤ 10 ps.

TABLE 3: Photophysical Properties of 5–7 in Several Solvents

BODIPY	solvent ^a	λ_{abs} (max/nm)	λ_{em} (max/nm)	λ_{ex} (max/nm)	fwhm(abs) (cm ⁻¹)	$\Delta\bar{\nu}$ (cm ⁻¹)	ϕ_{f}	τ^b (ns)	k_{f} (10 ⁸ s ⁻¹)	k_{nr} (10 ⁸ s ⁻¹)
5	toluene	534	558	534	1431	805	0.13			
	CHCl ₃	532	555	532	1560	779	0.095			
	cyclohexane	530	553	530	1331	785	0.076			
	1,4-dioxane	531	554	531	1599	782	0.079			
	THF	530	555	530	1442	850	0.084			
	EtOAc	527	551	527	1624	827	0.046			
	MeOH	525	549	525	1516	833	0.037			
6	toluene	557	589	557	1507	975	0.42	2.17	1.9	2.7
	CHCl ₃	554	588	554	1632	1044	0.31	1.97	1.6	3.5
	cyclohexane	553	585	553	1457	989	0.31	1.56	2.0	4.4
	1,4-dioxane	552	587	552	1529	1080	0.25	1.59	1.6	4.7
	THF	553	586	553	1626	1018	0.22	1.40	1.6	5.6
	EtOAc	549	583	549	1687	1062	0.20	1.37	1.5	5.8
	MeOH	547	582	547	1625	1100	0.21	1.22	1.7	6.5
7	toluene	534	558	534	1465	805	0.51	2.51	2.0	2.0
	CHCl ₃	530	557	530	1448	915	0.38	2.49	1.5	2.5
	cyclohexane	532	553	532	1254	714	0.28	1.50	1.9	4.8
	1,4-dioxane	529	556	529	1526	918	0.36	2.25	1.6	2.9
	THF	528	555	528	1532	921	0.30	1.78	1.7	3.9
	EtOAc	526	552	526	1476	895	0.28	1.68	1.7	4.3
	MeOH	523	550	523	1841	939	0.23	1.54	1.5	4.9

^a The solvents are ordered according to decreasing polarizability (with the refractive index n as criterion). ^b The standard errors on all lifetimes τ are ≤ 10 ps.

acid (see section 2.2). In the past, 3,5-diaryl-4,4-difluoro-4-bora-3a,4a-diaza-*s*-indacene dyes have been synthesized by condensation of 2-arylpurroles with suitably substituted benzoyl chlorides and incorporation of the boron difluoride entity.^{23,24,25}

Compounds 5–7 show the typical absorption and emission features of BODIPY,^{8,14–18} that is, a narrow absorption band with a maximum in the 523–534 nm range for the monoaryl derivatives 5 and 7 and 547–557 nm for the 3,5-diaryl compound 6, assigned to the S₀–S₁ transition. As before, disubstitution (in 6) shifts the absorption maxima to the red (by ~20 nm) compared to the monoaryl-substituted analogs (5 and 7). An additional, weaker, broad absorption band, attributed to the S₀–S₂ transition, is observed at the short-wavelength side. The absorption spectral bandwidths fwhm(abs) of the aryl-substituted dyes [the average fwhm(abs) values obtained in the various solvents are the following: fwhm(abs) = (1.5 ± 0.1) × 10³ cm⁻¹ for 5; fwhm(abs) = (1.6 ± 0.1) × 10³ cm⁻¹ for 6; fwhm(abs) = (1.5 ± 0.2) × 10³ cm⁻¹ for 7] are broader than for the ethynylaryl (1, 2) and ethenylaryl (3, 4) derivatives. For each of the aryl-substituted dyes 5–7, there is no systematic trend in fwhm(abs) as a function of solvent, except for the consistently smaller value fwhm(abs) observed in cyclohexane. The emission maxima of 3,5-diarylBODIPY 6 (~586 nm) are red-shifted by approximately 30 nm compared with 5 and 7.

The fluorescence emission spectra are mirror images of the absorption spectra. The Stokes shifts $\Delta\bar{\nu}$ of 5–7 are two to three times larger than those of 1–4. The $\Delta\bar{\nu}$ values of 6 are generally larger than those of 5. This diverges from the behavior observed for 4 and 2 where no difference with respectively 3 and 1 was observed. The larger Stokes shifts indicate a larger change of some equilibrium coordinates in S₁ (possibly the dihedral angle between the aryl groups and the BODIPY core). The quantum yields of 6 and 7 are moderately high (0.2–0.5) and become steadily smaller in more polar solvents, while those for 5 are low ($\phi_{\text{f}} \leq 0.13$). Table 3 summarizes the spectroscopic and photophysical data for 5–7 in several solvents.

Introduction of one aryl substituent at position 3 in 5 causes red shifts in both the absorption (excitation) and emission spectra by approximately 20 and 30 nm, respectively, compared to dichloroBODIPY 8.¹⁷ The absorption and emission spectral maxima of the 3-aryl derivatives 5 and 7 are, in general, very alike and show similar solvent-dependent behavior (see next section).

Dye 5 exhibits the lowest quantum yield among the dyes 1–7. Increasing the electron-donating strength of the group at position 3 (or 5) (methoxy in 7 vs chloro in 5) does not cause a spectral shift in the absorption and the fluorescence band but leads to higher ϕ_{f} values. The highest lifetimes of 6 and 7 were found

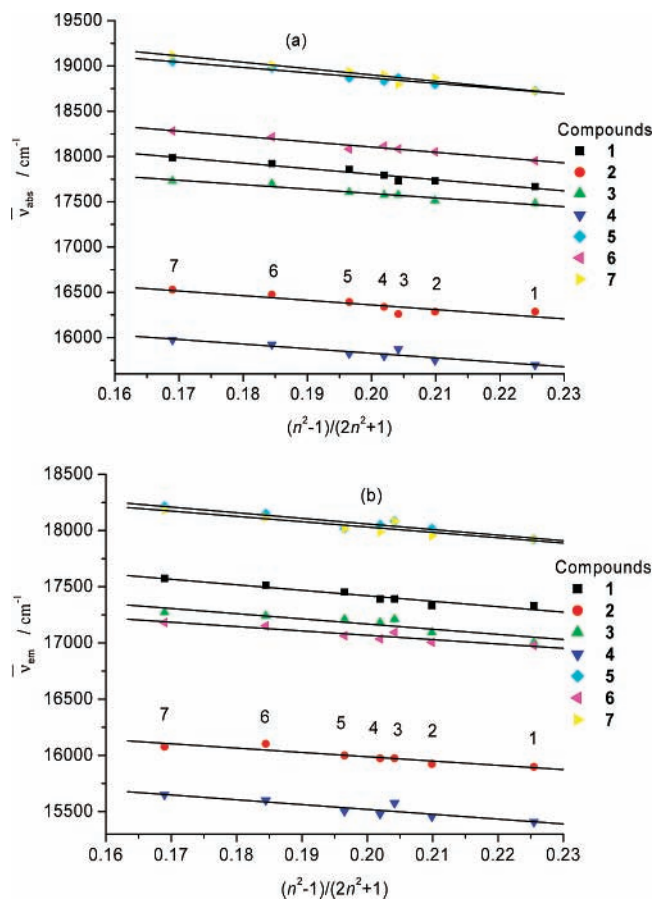


Figure 4. Plots of (a) the absorption maxima $\bar{\nu}_{\text{abs}}$ and (b) fluorescence emission maxima $\bar{\nu}_{\text{em}}$ for compounds 1–7 vs $f(n^2) = (n^2 - 1)/(2n^2 + 1)$ as a function of solvent: 1 = toluene (1.494); 2 = chloroform (1.444); 3 = cyclohexane (1.427); 4 = 1,4-dioxane (1.420); 5 = tetrahydrofuran (THF) (1.404); 6 = ethyl acetate (1.370); 7 = methanol (1.329). The numbers between parentheses are the n values. The r (correlation coefficient) values for the $\bar{\nu}_{\text{abs}}$ plots (a) for 1–7 are 0.971, 0.904, 0.976, 0.940, 0.985, 0.981, and 0.964, respectively. The corresponding r values for the $\bar{\nu}_{\text{em}}$ plots (b) are 0.961, 0.926, 0.902, 0.904, 0.946, 0.940, and 0.915, respectively.

in the most polarizable solvents toluene and chloroform. The fluorescence quantum yields and lifetimes of **6** and **7** decrease when the solvent is changed from toluene to methanol. For **6** and **7**, the k_f values in the various solvents calculated according to eq 2 yield a mean value of $(1.7 \pm 0.2) \times 10^8 \text{ s}^{-1}$. Parallel to the larger values of $\text{fwhm}(\text{abs})$ and $\Delta\bar{\nu}$, the larger k_{nr} values reflect a larger exciton phonon coupling, possibly for the libration of the 3-substituent.

3.4. Solvatochromism of Compounds 1–7. In Figure 4 the maxima of the absorption ($\bar{\nu}_{\text{abs}}$) and fluorescence ($\bar{\nu}_{\text{em}}$) bands of 1–7 are plotted against the solvent parameter $f(n^2) = (n^2 - 1)/(2n^2 + 1)$. The linearity of the plots of $\bar{\nu}_{\text{abs}}$ and $\bar{\nu}_{\text{em}}$ vs $f(n^2)$ confirms that Van der Waals and excitonic interactions with a polarizable solvent can rationalize the solvent dependence of the excitation energy.²⁶ If a large difference in permanent dipole moment would exist between the ground and excited state, the excitation energy would depend linearly on $\Delta f = f(\epsilon) - f(n^2) = [(\epsilon - 1)/(2\epsilon + 1)] - [(n^2 - 1)/(2n^2 + 1)]$ rather than on $f(n^2)$ and, hence, no linear dependence on $f(n^2)$ would be observed anymore. The near-independence of the Stokes shift $\Delta\bar{\nu}$ of each dye upon the solvent polarity $[(4.0 \pm 0.3) \times 10^2 \text{ cm}^{-1}$ for **1**, $(3.8 \pm 0.5) \times 10^2 \text{ cm}^{-1}$ for **2**, $(4.2 \pm 0.4) \times 10^2 \text{ cm}^{-1}$ for **3**, $(3.1 \pm 0.2) \times 10^2 \text{ cm}^{-1}$ for **4**, $(8.1 \pm 0.3) \times 10^2 \text{ cm}^{-1}$ for **5**, $(10.4 \pm 0.5) \times 10^2 \text{ cm}^{-1}$ for **6**, and $(8.7 \pm 0.8) \times 10^2 \text{ cm}^{-1}$ for **7**] also indicates that the permanent dipole

TABLE 4: Redox potentials (in V) vs Ag/AgCl of Compounds 1–7^a

BODIPY	E_{ox} (V)	E_{red} (V)
1	+1.52 ^b	−0.71
2	+1.02	−0.62
3	+1.36 ^b	−0.84 ^c
4	+1.02	−0.85
5	+1.60 ^b	−0.81
6	+1.31	−0.85
7	+1.21 ^b	−1.14 ^c

^a Experiments conducted in 0.1 M solutions of (TBA)PF₆ in CH₂Cl₂ at 200 mV s^{−1}. All solutions were purged with argon prior to measurement. The cell consisted of platinum working and counter electrodes and an Ag/AgCl reference electrode. ^b Irreversible oxidation process. ^c Irreversible reduction process.

moments (if any) do not differ between the ground state and the excited state.^{27,28} The slopes of all curves in Figure 4 for 1–7 are very similar, indicating that the spectral characteristics of all dyes react in a comparable way to changes of solvent polarizability. The near-coincidence of the plots for **5** and **7** implies that the spectral maxima $\bar{\nu}_{\text{abs}}$ and $\bar{\nu}_{\text{em}}$ are independent of the chloro or methoxy substituent.

3.5. Electrochemistry. The redox properties of 1–7 are shown in Table 4. When one compares the asymmetric dyes **1**, **3**, and **5** with their symmetric analogues, the most dramatic and relevant differences are manifested in their oxidation potentials. Derivatives **1** and **2** show a large difference in their oxidation potentials (~500 mV). This clearly demonstrates that the substitution of the second electron-donating ethynylphenyl group at the 3-position of **2** renders oxidation of this compound more facile than that of **1**, which contains the electron-withdrawing chlorine atom at the same position. A similar effect is observed when comparing dyes **3** and **4** where the addition of a second styryl substituent to **4** shifts oxidation by ~300 mV more negatively with respect to **3**. Finally, this trend is again observed in compounds **5**–**7**. Adding a second phenyl substituent to **6** shifts oxidation by ~300 mV more negatively with respect to **5**; the substitution of chlorine atom for the methoxy group in **7** shifts oxidation by ~400 mV more negatively with respect to **5**. This last observation is in line with the increased electron-donating capacity of the methoxy substituent compared to the phenyl group.

As regards the reduction potentials listed in Table 4, the asymmetric dyes **1**, **3**, and **5** show negligible differences when compared to their symmetrical analogues **2**, **4**, and **6**. The methoxy group in **7**, in addition to shifting the oxidation potential negatively when compared to **5**, also shifts the reduction potential more negatively to a similar degree.

3.6. Quantum-Chemical Calculations. The spectroscopic properties (absorption and emission vertical transition energies and radiative lifetimes) calculated at the INDO/SCI level for compounds 1–8 are compared to experiment in Figure 5. The quantum-chemical results fully support the experimental findings above:

(i) The optical transition is red-shifted when the chlorine atoms are substituted by one/two of the side groups investigated here. The red shift upon substitution increases in the order phenyl < ethynylphenyl < styryl. Disubstituted compounds show lower electronic transition energies than their corresponding monosubstituted counterparts. Such a bathochromic shift is attributed to an extension of the π -system and is the most effective for the styryl moieties. The delocalization of the electronic excitation over the side groups can better be appreciated from the transition density distributions displayed in Figure 6. Note that the lower shifts calculated for the phenyl derivatives

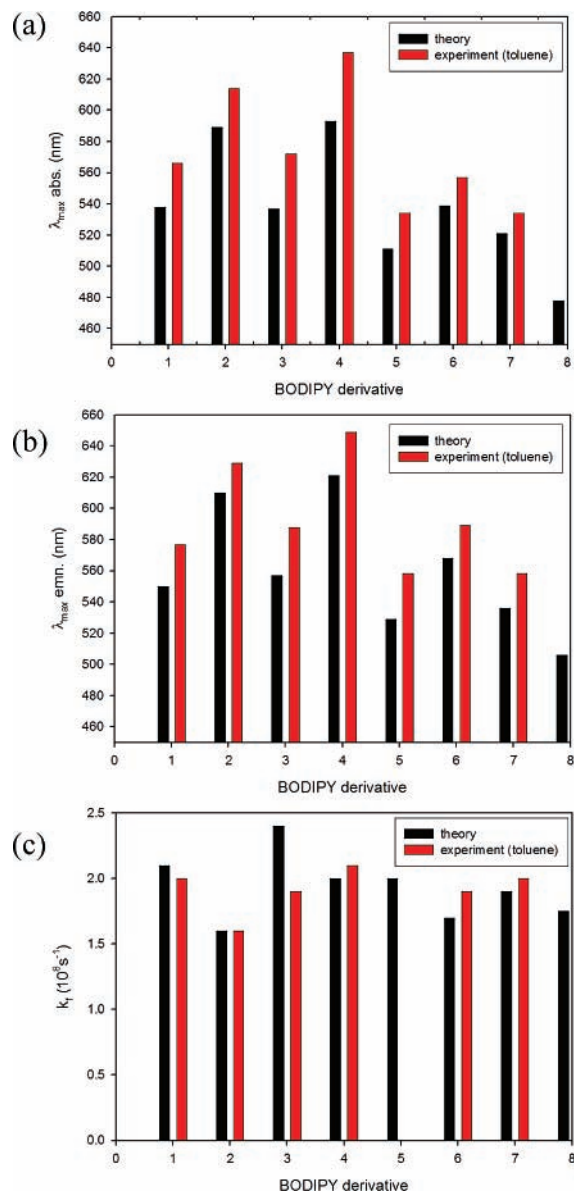


Figure 5. Comparison between calculated (INDO/SCI) and experimental (a) absorption and (b) emission wavelengths at maximum intensity and (c) radiative decay rate constants in compounds 1–8.

also stem from conformational effects: the dihedral angle between the phenyl ring and the BODIPY core amounts to 50° in the ground-state (GS) geometry and 30° in the excited-state (ES) geometry, compared to 9° (GS) and 1° (ES) for the ethynylphenyl and 10° (GS) and 7° (ES) for the styryl compounds. This reflects the observations made when comparing fwhm(abs), $\Delta\bar{\nu}$, and k_{nr} between the three series (1, 2; 3, 4; 5–7).

(ii) The computed radiative decay rate constants are in the range $(1.5\text{--}2.5) \times 10^8 \text{ s}^{-1}$ for all compounds investigated. As shown in eq 4, the radiative rate constant depends both on the excitation energy and the transition dipole moment. The latter steadily increases upon substituting one chlorine with a phenyl, an ethynylphenyl, and a styryl moiety. This effect results from both a reshuffling in the electronic density over the BODIPY core in the asymmetric molecules and the delocalization of the π -electronic cloud over the side group (Figure 6). However, the transition dipole moment is hardly affected upon adding a second branch to the BODIPY core, despite the fact that significant transition densities are computed on both branches (likely because this is counterbalanced by smaller contributions

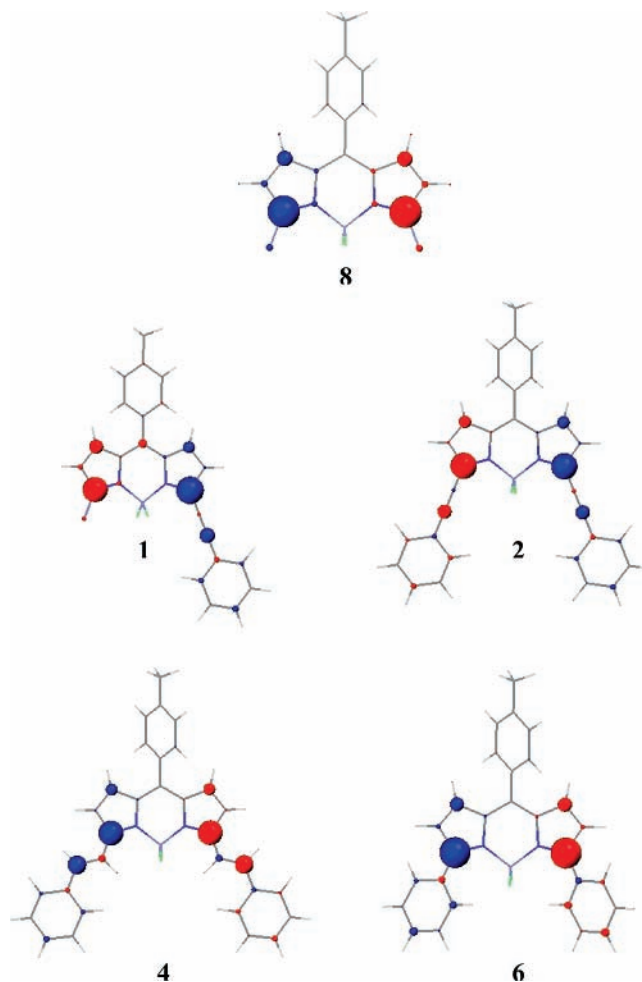


Figure 6. Transition densities computed for the lowest optical excitation in the BODIPY derivatives studied.

over the BODIPY unit in the 3,5-disubstituted molecules). As a result, the radiative decay rate constant increases from 8 to 1 but decreases from 1 to 2 in spite of the continuous decrease in excitation energy in the series $8 \rightarrow 1 \rightarrow 2$. Note that a similar trend is calculated for the other two series, $8 \rightarrow 3 \rightarrow 4$ and $8 \rightarrow 5 \rightarrow 6$. This follows exactly the experimental findings for the series $8 \rightarrow 1 \rightarrow 2$, yet the INDO/SCI calculations yield a relative order in the radiative decay rate constants for 3 and 4 that is opposite to the experimental result.

The computed redox properties—namely the shifts in the HOMO and LUMO levels computed for dyes 1–7 in comparison to 8 (taken as a reference)—are in qualitative agreement with the experimental measurements. Substitution of the chlorine atoms at the 3(5)-position(s) of 8 leading to compounds 1–7 results in an asymmetric destabilization of the HOMO and LUMO orbitals, with a larger effect calculated for the HOMO. Thus, in the 3(5)-substituted dyes 1–7, the side groups act as electron donors. The addition of a second substituent leads to a larger variation in HOMO energies (by 0.4–0.5 eV) compared to the LUMO (by 0.1–0.2 eV) (see Table 5). This can be attributed to an extension of the π -system, which is more efficient for the HOMO owing to larger weights in 3,5 positions compared to the LUMO; see Figure 7. The calculations clearly show the shift of the LUMO energy of 7.

4. Conclusion

A series of 3-phenyl-, 3-styryl-, and 3-ethynylphenylboronazaindane dyes and their corresponding 3,5-disubstituted

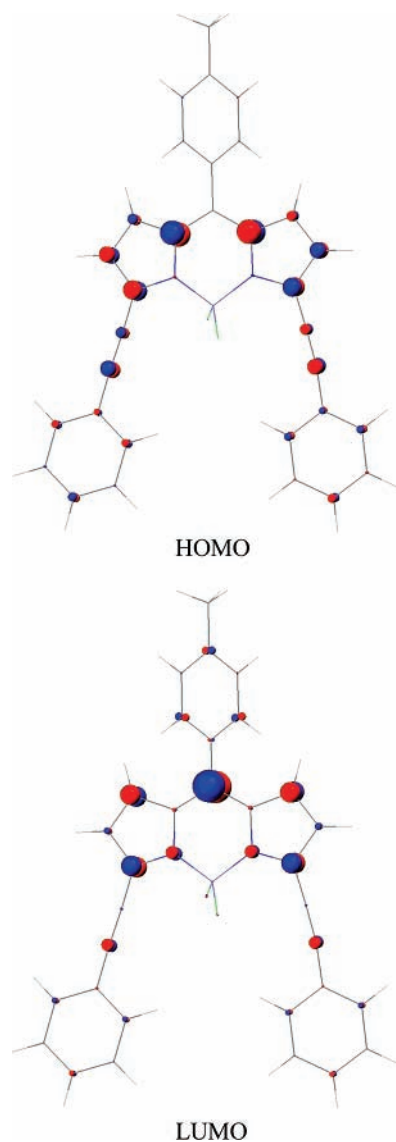


Figure 7. Bonding–antibonding pattern in the HOMO and LUMO levels of molecule 2.

TABLE 5: Δ HOMO and Δ LUMO of Compounds 1–7 Compared to 8

BODIPY	Δ HOMO (meV)	Δ LUMO (meV)
1	510	97
2	929	214
3	537	85
4	1005	191
5	323	153
6	711	349
7	746	505

analogs have been synthesized via palladium-catalyzed coupling reactions with the appropriate 3,5-dichloroBODIPY. Structural modification of the difluoroboradipyrromethene core via conjugation-extending residues at the 3- (or 3,5-) position(s) significantly affects the spectroscopic and photophysical properties of the BODIPY fluorophore. The absorption and fluorescence emission spectral maxima of the studied BODIPY derivatives range from green to near-infrared, with the disubstituted compounds showing significant red shifts compared to their monosubstituted analogs. The extremely bright dyes **1** and **2** are the first representatives of BODIPY dyes with ethynylaryl substituents at the 3(5)-position(s). Quantum-chemical calculations reveal that the characteristics of the lowest optically

allowed excited state is very sensitive to both the nature and the position of the substituent. Compounds **1** and **2** shift the spectral maxima to longer wavelengths compared to the related aryl-substituted **5–7** but to a lesser degree than the vinylaryl derivatives **3** and **4**. Indeed, introduction of styryl substituents (at the 3-position in **3** and at the 3,5-positions in **4**) causes the largest bathochromic shift in both the absorption and emission spectra because of the extension in the π -delocalized system. The quantum yields of **1–4** are significantly higher than those of the aryl-substituted dyes **5–7**. Additionally, electrochemical measurements show large differences between the asymmetric and symmetric dyes in their oxidation potentials (300–500 mV), indicating the ease with which the energy levels of these compounds can be manipulated via substitution at the 3,5-positions. The novel ethynylaryl-substituted boradiazaindacene fluorophores combine extremely high fluorescence quantum yields and long lifetimes with emission spectra extending into the near-infrared spectral region. We believe that their remarkable spectroscopic and photophysical properties will lead to useful applications in the future.

Acknowledgment. This research is supported partly by the IAP-V-03 and IAP-VI-27 programs, which also provided a fellowship to W.Q. We thank the Instituut voor Wetenschappelijk Technisch Onderzoek (IWT) for Grant ZWAP 04/007. The University Research Fund of the K.U. Leuven is thanked for Grant GOA 2001/2 and fellowships to T.R. and J.N.C. We are grateful to Dr. M. Sliwa and Mr. P. Dedecker for technical help with the single-photon timing measurements. D.B. is a Research Associate of the Belgian National Fund for Scientific Research (FNRS). B.V.A. acknowledges a grant from the Fonds pour la formation à la Recherche dans l'Industrie et dans l'Agriculture (FRIA).

References and Notes

- (1) (a) Czarnik, A. W. *Fluorescent Chemosensors for Ion and Molecule Recognition*; American Chemical Society: Washington, DC, 1993. (b) de Silva, A. P.; Gunaratne, H. Q. N.; Gunnlaugsson, T.; Huxley, A. J. M.; McCoy, C. P.; Rademacher, J. T.; Rice, T. E. *Chem. Rev.* **1997**, *97*, 1515–1566.
- (2) Treibs, A.; Kreuzer, F.-H. *Liebigs Ann. Chem.* **1968**, *718*, 208–223.
- (3) Ziessel, R.; Ulrich, G.; Harriman, A. *New J. Chem.* **2007**, *31*, 496–501.
- (4) Haugland, R. P. *The Handbook. A Guide to Fluorescent Probes and Labeling Technologies*, 10th ed.; Molecular Probes: Eugene, OR, 2005.
- (5) (a) Baruah, M.; Qin, W.; Vallée, R. A. L.; Beljonne, D.; Rohand, T.; Dehaen, W.; Boens, N. *Org. Lett.* **2005**, *7*, 4377–4380. (b) Rohand, T.; Baruah, M.; Qin, W.; Boens, N.; Dehaen, W. *Chem. Commun.* **2006**, 266–268.
- (6) Rohand, T.; Qin, W.; Boens, N.; Dehaen, W. *Eur. J. Org. Chem.* **2006**, 4658–4663.
- (7) Olmsted, J. *J. Phys. Chem.* **1979**, *83*, 2581–2584.
- (8) Qin, W.; Baruah, M.; Van der Auweraer, M.; De Schryver, F. C.; Boens, N. *J. Phys. Chem. A* **2005**, *109*, 7371–7384.
- (9) (a) O'Connor, D. V.; Phillips, D. *Time-correlated Single Photon Counting*; Academic Press: New York, 1984. (b) vandeVen, M.; Ameloot, M.; Valeur, B.; Boens, N. *J. Fluoresc.* **2005**, *15*, 377–413. (c) Boens, N.; Qin, W.; Basarić, N.; Hofkens, J.; Ameloot, M.; Pouget, J.; Lefèvre, J.-P.; Valeur, B.; Gratton, E.; vandeVen, M.; Silva, N. D.; Engelborghs, Y.; Willaert, K.; Sillen, A.; Rumbles, G.; Phillips, D.; Visser, A. J. W. G.; Van Hoek, A.; Lakowicz, J. R.; Malak, H.; Gryczynski, I.; Szabo, A. G.; Krajcarski, D. T.; Tamai, N.; Miura, A. *Anal. Chem.* **2007**, *79*, 2137–2149.
- (10) Crovetto, L.; Orte, A.; Talavera, E. M.; Alvarez-Pez, J. M.; Cotlet, M.; Thielemans, J.; De Schryver, F. C.; Boens, N. *J. Phys. Chem. B* **2004**, *108*, 6082–6092.
- (11) Van den Zegel, M.; Boens, N.; Daems, D.; De Schryver, F. C. *Chem. Phys.* **1986**, *101*, 311–335.
- (12) Dewar, M. J. S.; Zoebisch, E. G.; Healy, E. F.; Stewart, J. J. P. *J. Am. Chem. Soc.* **1985**, *107*, 3902–3909.
- (13) Zerner, M. C. In *Reviews in Computational Chemistry*; Lipkowitz, K. W., Boyd, D. B., Eds.; VCH: New York, 1991; Vol. 2, pp 313–365.

- (14) Vos de Wael, E.; Pardoën, J. A.; van Koeveringe, J. A.; Lugtenburg, J. *Recl. Trav. Chim. Pays-Bas* **1997**, *96*, 306–309.
- (15) Kollmannsberger, M.; Rurack, K.; Resch-Genger, U.; Daub, J. *J. Phys. Chem. A* **1998**, *102*, 10211–10220.
- (16) (a) López Arbeloa, T.; López Arbeloa, F.; López Arbeloa, I.; García-Moreno, I.; Costela, A.; Sastre, R.; Amat-Guerri, F. *Chem. Phys. Lett.* **1999**, *299*, 315–321. (b) Costela, A.; García-Moreno, I.; Gomez, C.; Sastre, R.; Amat-Guerri, F.; Liras, M.; López Arbeloa, F.; Bañuelos Prieto, J.; López Arbeloa, I. *J. Phys. Chem. A* **2002**, *106*, 7736–7742. (c) López Arbeloa, F.; Bañuelos Prieto, J.; Martínez Martínez, V.; Arbeloa López, T.; López Arbeloa, I. *Chem. Phys. Chem.* **2004**, *5*, 1762–1771. (d) Bañuelos Prieto, J.; López Arbeloa, F.; Martínez Martínez, V.; Arbeloa López, T.; Amat-Guerri, F.; Liras, M.; López Arbeloa, I. *Chem. Phys. Lett.* **2004**, *385*, 29–35.
- (17) Qin, W.; Rohand, T.; Baruah, M.; Stefan, A.; Van der Auweraer, M.; Dehaen, W.; Boens, N. *Chem. Phys. Lett.* **2006**, *420*, 562–568.
- (18) (a) Baruah, M.; Qin, W.; Basarić, N.; De Borggraeve, W. M.; Boens, N. *J. Org. Chem.* **2005**, *70*, 4152–4157. (b) Qin, W.; Baruah, M.; Stefan, A.; Van der Auweraer, M.; Boens, N. *Chem. Phys. Chem.* **2005**, *6*, 2343–2351.
- (19) Ziessel, R.; Goze, C.; Ulrich, G.; Césarío, M.; Retailleau, P.; Harriman, A.; Rostron, J. P. *Chem.—Eur. J.* **2005**, *11*, 7366–7378.
- (20) Ulrich, G.; Goze, C.; Guardigli, M.; Roda, A.; Ziessel, R. *Angew. Chem., Int. Ed.* **2005**, *44*, 3694–3698.
- (21) (a) Rurack, K.; Kollmannsberger, M.; Daub, J. *Angew. Chem., Int. Ed.* **2001**, *40*, 385–387. (b) Coskun, A.; Akkaya, E. U. *J. Am. Chem. Soc.* **2005**, *127*, 10464–10465. (c) Baruah, M.; Qin, W.; Flors, C.; Hofkens, J.; Vallée, R. A. L.; Beljonne, D.; Van der Auweraer, M.; De Borggraeve, W. M.; Boens, N. *J. Chem. Phys. A* **2006**, *110*, 5998–6009. (d) Qin, W.; Baruah, M.; De Borggraeve, W. M.; Boens, N. *J. Photochem. Photobiol. A: Chem.* **2006**, *183*, 190–197. (e) Peng, X.; Du, J.; Fan, J.; Wang, J.; Wu, Y.; Zhao, J.; Sun, S.; Xu, T. *J. Am. Chem. Soc.* **2007**, *129*, 1500–1501.
- (22) Rurack, K.; Kollmannsberger, M.; Daub, J. *New. J. Chem.* **2001**, *25*, 289–292.
- (23) Thoresen, L. H.; Kim, H.; Welch, M. B.; Burghart, A.; Burgess, K. *Synlett* **1998**, 1276.
- (24) Burghart, A.; Kim, H.; Welch, M. B.; Thoresen, L. H.; Reibenspies, J.; Burgess, K. *J. Org. Chem.* **1999**, *64*, 7813–7819.
- (25) Kim, H.; Burghart, A.; Welch, M. B.; Reibenspies, J.; Burgess, K. *Chem. Commun.* **1999**, 1889–1890.
- (26) Pevenage, D.; Corens, D.; Dehaen, W.; Van, der Auweraer, M.; De Schryver, F. C. *Bull. Soc. Chim. Belg.* **1997**, *106*, 565–572.
- (27) Lippert, E. *Z. Naturforsch., A: Phys. Sci.* **1955**, *10*, 541–545.
- (28) Mataga, N.; Kaifu, Y.; Koizumi, M. *Bull. Chem. Soc. Jpn.* **1955**, *28*, 690–691; **1956**, *29*, 465–470.